entropy

MDPI

Article

Multipartite Entanglement: A Journey through Geometry

Songbo Xie *, Daniel Younis, Yuhan Mei and Joseph H. Eberly *

Center for Coherence and Quantum Optics, Department of Physics and Astronomy, University of Rochester, Rochester, NY 14627, USA; dan.younis@outlook.com (D.Y.)
* Correspondence: sxie9@ur.rochester.edu (S.X.); eberly@pas.rochester.edu (J.H.E.)

Abstract: Genuine multipartite entanglement is crucial for quantum information and related technologies, but quantifying it has been a long-standing challenge. Most proposed measures do not meet the "genuine" requirement, making them unsuitable for many applications. In this work, we propose a journey toward addressing this issue by introducing an unexpected relation between multipartite entanglement and hypervolume of geometric simplices, leading to a tetrahedron measure of quadripartite entanglement. By comparing the entanglement ranking of two highly entangled four-qubit states, we show that the tetrahedron measure relies on the degree of permutation invariance among parties within the quantum system. We demonstrate potential future applications of our measure in the context of quantum information scrambling within many-body systems.

Keywords: genuine multipartite entanglement; entanglement measure; geometric measure; triangle measure; tetrahedron measure; entanglement entropy; entanglement polygon inequalities; entropic fill; permutation invariance; information scrambling

check for updates

Citation: Xie, S.; Younis, D.; Mei, Y.; Eberly, J.H. Multipartite Entanglement: A Journey through Geometry. *Entropy* **2024**, *26*, 217. https://doi.org/10.3390/e26030217

Academic Editors: Syed Assad and Jie Zhao

Received: 30 January 2024
Revised: 21 February 2024
Accepted: 28 February 2024
Published: 29 February 2024

Copyright: © 2024 by the authors. Licensee MDPI, Basel, Switzerland. This article is an open access article distributed under the terms and conditions of the Creative Commons Attribution (CC BY) license (https://creativecommons.org/licenses/by/4.0/).

1. Introduction

Genuine multipartite entanglement (GME) is a form of entanglement beyond two parties, offering distinct advantages over two-party entanglement [1]. The primary benefit of GME lies in its capacity to facilitate complex quantum tasks [2–4]. Consequently, comprehending GME in many-body systems is valuable for the development of quantum technologies.

An entanglement measure is necessary to quantify the amount of entanglement. Entanglement measures are vital in various actions, including investigating the dynamical behavior of many-body systems, quantifying the performance of quantum protocols, and identifying the nature of phase transitions in many-body systems [5–8]. The "genuine" requirement requires that a GME measure should only, and always, vanish for biseparable states [9,10]. Essentially, a GME measure should quantify the degree of nonbiseparability among multi-party quantum states. This is crucial to quantify accurately the collective strength of the parties' entanglement and unlock their potential in quantum tasks.

Unfortunately, many proposed multipartite entanglement measures, including some extensively used [11–14], fail to meet the "genuine" requirement, making them unsuitable in many practical applications. One popular route to construct a GME measure is to use distance-based approaches, including relative entropy [15] and some "geometric measures" [16–18]. However, evaluating such measures requires using optimization procedures, which is highly challenging, sometimes even for pure states.

In this work, to solve this measure-identification problem, we embark on a distinct journey. The journey begins with the triangle measure for three-qubit systems that we introduced recently [10]. However, extending this measure to systems with more than three qubits is challenging due to the over-flexibility of geometric shapes. Various attempts have been made, but they either fail to meet the "genuine" requirement or lose simple geometric intuition [19–21].

We demonstrate the possibility of a "geometric journey" by presenting a tetrahedron measure for four-qubit systems. We show that our novel method, even though sharing the

same term "geometry" with distance-based measures, presents fundamental distinctions by offering an unexpected connection between multipartite entanglement and hypervolume of geometric simplices. It also relies on the degree of permutation invariance among parties within the quantum system—a feature not shared by the distance-based measures. This promises future avenues, for example, for investigating information scrambling in many-body systems.

2. From Three to Four

Von Neumann entropy is crucial in our approach. Specifically, the entanglement E of a bipartite pure quantum state ψ_{12} can be characterized by the von Neumann entropy S of either of the individual parties, $E(\psi_{12}) := S(\rho_i) \equiv -\mathrm{Tr}(\rho_i \log_2 \rho_i)$, where ρ_i is the reduced density operator of the party i. $E(\psi_{12})$ is called *entanglement entropy* of the state ψ_{12}.

Other crucial ingredients are the "entanglement polygon inequalities" [22]. Specifically, for a general n-qubit system, when entanglement entropy is considered between one qubit and the remaining $(n-1)$ qubits, we obtain n one-to-other bipartite entropies. The entanglement polygon inequalities require that any one of them cannot exceed the sum of the other $(n-1)$ values. For a three-qubit state, these relations hold $E_{i(jk)} \leq E_{j(ki)} + E_{k(ij)}$. Here, $E_{i(jk)} := S(\rho_i)$, where the subscript i refers to the system's ith qubit, and $\{i, j, k\}$ is any permutation of $\{1, 2, 3\}$.

Those inequalities can be geometrically interpreted as the three one-to-other entropies representing the lengths of the three edges of a triangle. We demonstrated that the area of this triangle can measure three-qubit GME, with squared concurrence being employed in lieu of entanglement entropy [10,23]. We now illustrate that entanglement entropy offers distinct advantages.

The inequalities for four-qubit systems are [22]

$$E_{i(jkl)} \leq E_{j(kli)} + E_{k(lij)} + E_{l(ijk)}, \tag{1}$$

with $\{i, j, k, l\}$ being any permutation of $\{1, 2, 3, 4\}$. As suggested in [22], Equation (1) induces a quadrilateral, with the four edge lengths equal to the four one-to-other entropies. Therefore, following from the triangle measure in [10], a tempting candidate of a four-qubit GME measure is the area of this quadrilateral.

However, using the quadrilateral defined above poses problems. Firstly, since entanglement is invariant under qubit permutations, the four one-to-other entropies $E_{i(jkl)}$ must be treated equally. However, the four edges of a quadrilateral are not necessarily equal. A quadrilateral with different edge lengths can be arranged in three different ways, as shown in Figure 1. Furthermore, a quadrilateral has five degrees of freedom, while the edge lengths fix only four of them. Consequently, even if the four edge lengths are fixed, the area of the quadrilateral can still vary, rendering the entanglement measure undetermined.

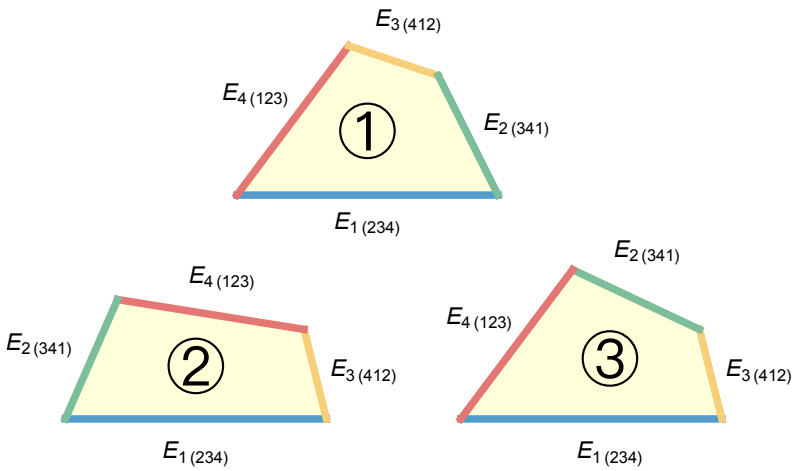

Figure 1. The interpretation of Equation (1) as a quadrilateral violates the invariance of entanglement under qubit permutations since the four edges are not treated equally, resulting in three distinct possible quadrilaterals. Here, edges of the same color indicate equal length.

3. From Polygon to Simplex

Instead, we consider an "entropic tetrahedron" induced by Equation (1), of which the four face areas are equal to the four one-to-other entropies. The advantage of this tetrahedron approach quickly becomes apparent when one observes that the four faces are treated equally. We reinterpret the results of [22] in this new framework as *entanglement simplex inequalities*, where the term "simplex" generalizes the notions of triangle and tetrahedron to arbitrary dimensions.

Before proceeding, it is important to note that a tetrahedron has six degrees of freedom, while the four face areas fix only four of them. Consequently, if we attempt to employ the entropic tetrahedron's volume to measure GME, it remains undetermined.

To further elaborate, we note that every tetrahedron has a unique inscribed sphere tangent to all four faces. For each face, one can connect the point of contact with the inscribed sphere to the three vertices, which divides the face into three smaller triangles. The twelve smaller triangles on the four faces are related pairwise: any two triangles that share an edge of the tetrahedron have the same area. The six different areas of the smaller triangles are labeled $\{\sigma_{12}, \sigma_{13}, \sigma_{14}, \sigma_{23}, \sigma_{24}, \sigma_{34}\}$, as shown in Figure 2. As a simple exercise, one can show that the areas of the smaller triangles fix the tetrahedron, whose volume is

$$\begin{aligned} V &= \frac{\sqrt{2}}{3} S^{1/2} (A_0 A_1 A_2 A_3)^{1/4}, \\ \text{with } A_0 &= +\sqrt{\sigma_{12}\sigma_{34}} + \sqrt{\sigma_{13}\sigma_{24}} + \sqrt{\sigma_{14}\sigma_{23}}, \\ A_1 &= -\sqrt{\sigma_{12}\sigma_{34}} + \sqrt{\sigma_{13}\sigma_{24}} + \sqrt{\sigma_{14}\sigma_{23}}, \\ A_2 &= +\sqrt{\sigma_{12}\sigma_{34}} - \sqrt{\sigma_{13}\sigma_{24}} + \sqrt{\sigma_{14}\sigma_{23}}, \\ A_3 &= +\sqrt{\sigma_{12}\sigma_{34}} + \sqrt{\sigma_{13}\sigma_{24}} - \sqrt{\sigma_{14}\sigma_{23}}. \end{aligned} \tag{2}$$

and $S = 2(\sigma_{12} + \sigma_{13} + \sigma_{14} + \sigma_{23} + \sigma_{24} + \sigma_{34})$, the total surface area of the entropic tetrahedron.

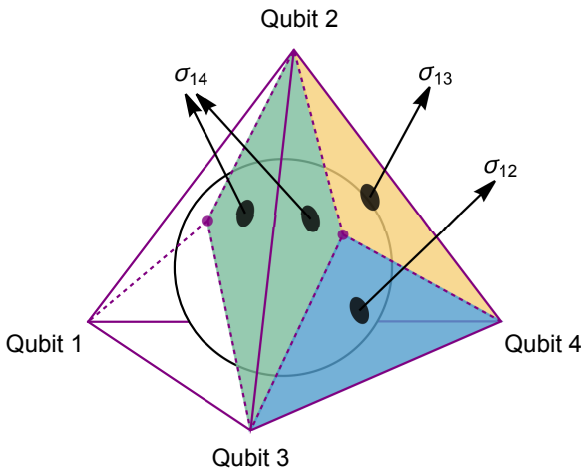

Figure 2. The inscribed sphere for a tetrahedron divides the four faces into twelve smaller triangles. Any two smaller triangles that share an edge of the tetrahedron exhibit identical areas, represented by the same color.

The six parameters $\{\sigma_{ij}\}$ must add up to the four face areas induced by the "entanglement simplex inequalities", given by (including four index permutations)

$$\sigma_{ij} + \sigma_{ik} + \sigma_{il} = E_{i(jkl)}. \tag{3}$$

However, these equations cannot fix the tetrahedron, as two more equations are required, and while the one-to-other entropies have been used so far, the construction of a four-qubit GME must also involve entropies representing two-to-other bipartitions, namely, $\{E_{(12)(34)}, E_{(13)(24)}, E_{(14)(23)}\}$, with $E_{(ij)(kl)} := S(\rho_{ij}) \equiv S(\rho_{kl})$, where the bipartitions separate the qubits into two groups of two.

On the one hand, if any one of the three two-to-other entanglement entropies vanishes, the state is biseparable. According to the "genuine" requirement, our proposed GME measure, the volume of the tetrahedron, should be zero. On the other hand, if any one of the three quantities A_1, A_2, and A_3 in Equation (2) vanishes, the tetrahedron's volume is also zero. To ensure consistency between these two conditions, we relate the quantities by the following Equations (including three index permutations):

$$-\sqrt{\sigma_{ij}\sigma_{kl}} + \sqrt{\sigma_{ik}\sigma_{jl}} + \sqrt{\sigma_{il}\sigma_{jk}} = \lambda \cdot E_{(ij)(kl)}. \tag{4}$$

The additional parameter λ can be canceled out when dividing the equations in (4) in pairs, leading to six equations for $\{\sigma_{ij}\}$ by combining Equations (3) and (4).

Equation (4) can be transformed to the quadratic form: $\sigma_{ij}\sigma_{kl} = (\lambda^2/4)[E_{(ik)(jl)} + E_{(il)(jk)}]^2$. Together with Equation (3), this simplifies the equations into one quartic equation for one single variable σ_{ij} with four distinct solutions. Importantly, this reasoning is universally applicable to all six $\{\sigma_{ij}\}$ due to their inherent symmetry. Consequently, a total of four sets of solutions exist for the six equations.

Our numerical investigations consistently confirm the presence of four distinct solution sets. Within these sets, there is one unique solution where all $\{\sigma_{ij}\}$ have non-negative values. Consequently, given an arbitrary four-qubit state, a tetrahedron can always be constructed where the areas of the six smaller triangles of the tetrahedron are equal to the non-negative values $\{\sigma_{ij}\}$. We call the construction an *entropic tetrahedron*.

4. Four-Qubit "Entropic Fill"

We introduce the four-qubit *entropic fill*, denoted as $F_4 := (3^{7/6}/2)V^{2/3}$, with V being the tetrahedron volume, given in Equation (2). The prefactor $3^{7/6}/2$ ensures the normalization $0 \leq F_4 \leq 1$. As will be explained, the exponent $2/3$ contributes to the additivity of F_4. We now prove that F_4 is a GME measure for four-qubit pure states.

(*A*) F_4 *satisfies the "genuine" requirement*—for an entanglement measure E to be "genuine", it is required that $E = 0$ for all biseparable states, and $E > 0$ for all nonbiseparable states [9,10]. We proceed to demonstrate that F_4 adheres to this "genuine" requirement.

For a four-qubit pure system, there are two types of biseparable states: one-to-other biseparable and two-to-other biseparable. In the case of one-to-other biseparable states, all four quantities A_0, A_1, A_2, and A_4 are zero, resulting in a tetrahedron with zero volume. For two-to-other biseparable states, one of the three quantities A_1, A_2, or A_3 is zero, leading to a tetrahedron with zero volume as well.

Conversely, if the volume of the constructed tetrahedron is zero, there are four possible scenarios, based on the expression of V in Equation (2):

- **Possibility** (a): $(A_1A_2A_3) = 0$, but A_1, A_2, and A_3 are not all zero. Without the loss of generality, we assume that $A_1 = 0$. According to Equation (4), this leads to $\lambda \neq 0$ and $E_{(12)(34)} = 0$, indicating that the state is at least two-to-other biseparable.
- **Possibility** (b): $A_0 = 0$. This is equivalent to $A_1 = A_2 = A_3 = 0$. In this scenario, it is easy to observe that $\sqrt{\sigma_{12}\sigma_{34}} = \sqrt{\sigma_{13}\sigma_{24}} = \sqrt{\sigma_{14}\sigma_{23}} = 0$. Therefore, at least one factor under each square root should be chosen to equal zero. We first assume that there exists a subscript i such that $\sigma_{ij} = \sigma_{ik} = \sigma_{il} = 0$. This leads to $E_{i(jkl)} = 0$, indicating that the state is at least one-to-other biseparable.
- **Possibility** (c): $A_0 = 0$, but the assumption in Possibility (b) is not valid. It can be shown that the only possibility to maintain each square root being zero is $\sigma_{jk} = \sigma_{kl} = \sigma_{lj} = 0$, while $\sigma_{ij} \neq 0$, $\sigma_{ik} \neq 0$, and $\sigma_{il} \neq 0$. The four face areas satisfy the relations $E_{i(jkl)} = E_{j(kli)} + E_{k(lij)} + E_{l(ijk)}$ with $E_{i(jkl)} > E_{j(kli)} > 0$, $E_{i(jkl)} > E_{k(lij)} > 0$, and $E_{i(jkl)} > E_{l(ijk)} > 0$, representing a tetrahedron with its four coplanar vertices. Using the same approach as in the appendix of [10], a contradiction can be shown. Therefore, this scenario does not exist for four-qubit systems.
- **Possibility** (d): $S = 0$. This implies that all $\{\sigma_{ij}\}$ are equal to zero. According to Equation (3), the state is a product state.

Therefore, we have demonstrated that the volume of the entropic tetrahedron assigned to a four-qubit state is zero if and only if the state is biseparable, demonstrating that F_4 satisfies the genuine requirement.

(*B*) F_4 *is additive*—an entanglement measure E is additive if $E(\psi^{\otimes n}) = nE(\psi)$, indicating that the entanglement of n identical copies of a state is n times the entanglement of a single copy [24].

With von Neumann entropy's additivity being a known fact, the quantities $\{E_{i(jkl)}, E_{(ij)(kl)}\}$ are all additive in Equations (3) and (4). Consequently, for n identical copies, the non-negative solutions of $\{\sigma_{ij}\}$ increase by a factor of n. This establishes the additivity of F_4 and justifies the essential inclusion of the exponent $2/3$ for V.

(*C*) *Local monotonicity*—an entanglement measure E should also satisfy local monotonicity, requiring that E is nonincreasing under local operations and classical communications (LOCC) [25]. For a general mixed state ρ, it means that $E(\rho) \geq E(\Lambda(\rho))$, where Λ is an arbitrary LOCC process [26]. For measures only defined for pure states, a stronger form of the requirement applies: $E(\psi) \geq \sum_i p_i E(\varphi_i)$, where $\{p_i, |\varphi_i\rangle\}$ is the ensemble obtained from $|\psi\rangle$ under LOCC [27].

We verify the local monotonicity of F_4 by adopting the numerical technique explained in [28]. In particular, as is shown in [1], it suffices to confine LOCC processes to positive-

operator-valued measures $\{X_1, X_2\}$ with binary outcomes, acting only on qubit 1. These operators satisfy the relation $X_1^\dagger X_1 + X_2^\dagger X_2 = \mathbb{I}$ and can be generally parameterized as

$$\begin{aligned} X_1 &= \begin{pmatrix} \sin\alpha_1 \cos\beta_1 & -e^{i\beta_2} \sin\alpha_1 \sin\beta_1 \\ \sin\alpha_2 \sin\beta_1 & e^{i\beta_2} \sin\alpha_2 \cos\beta_1 \end{pmatrix}, \\ X_2 &= \begin{pmatrix} \cos\alpha_1 \cos\beta_1 & -e^{i\beta_2} \cos\alpha_1 \sin\beta_1 \\ \cos\alpha_2 \sin\beta_1 & e^{i\beta_2} \cos\alpha_2 \cos\beta_1 \end{pmatrix}, \end{aligned} \tag{5}$$

with $\{\alpha_i, \beta_i\} \in [-\pi, \pi]$. Since entanglement measures are invariant under local unitary transformations, it suffices to confine the input state ψ to the generalized Schmidt form [29] as follows:

$$\begin{aligned} |\psi\rangle = {} & c_0|0000\rangle + c_4|0100\rangle + c_5|0101\rangle + c_6|0110\rangle \\ & + c_8|1000\rangle + c_9 e^{i\phi_1}|1001\rangle + c_{10} e^{i\phi_2}|1010\rangle \\ & + c_{11} e^{i\phi_3}|1011\rangle + c_{12} e^{i\phi_4}|1100\rangle + c_{13} e^{i\phi_5}|1101\rangle \\ & + c_{14} e^{i\phi_6}|1110\rangle + c_{15} e^{i\phi_7}|1111\rangle, \end{aligned} \tag{6}$$

with $\sum_i c_i^2 = 1$ and $\{\phi_i\} \in [0, \pi]$. The binary outcome states are given by $|\varphi_i\rangle = (X_i \otimes \mathbb{I} \otimes \mathbb{I} \otimes \mathbb{I})|\psi\rangle / \sqrt{p_i}$, and $\{p_i\}$ are normalization factors. Local monotonicity of F_4 is equivalent to the inequality

$$M(c_i, \phi_i, \alpha_i, \beta_i) := \left[F_4(\psi) - \sum_i \left(p_i F_4(\varphi_i) \right) \right] \geq 0. \tag{7}$$

We have conducted thorough numerical verifications, revealing that the minimum value of M among the 22 parameters is on the order of -10^{-6}. We emphasize that the numerical uncertainty associated with M, stemming from numerically solving Equations (3) and (4), is of a comparable magnitude, with $\Delta M \sim 10^{-6}$. To elaborate, we employ the propagation of uncertainty formula: $\Delta M = |\partial M / \partial \sigma_{ij}| \Delta \sigma_{ij}$, where $\Delta \sigma_{ij} \sim 10^{-15}$ arises from the double-precision format of σ_{ij}. Remarkably, our analysis indicates that $|\partial M / \partial \sigma_{ij}|$ can attain the order of 10^9, confirming the overall uncertainty in M as $\Delta M \sim 10^{-6}$. Therefore, the minimum value of M being -10^{-6} only reflects the systematic uncertainties embedded in the numerical computations.

For further validation, we fix the parameters $\{c_i, \phi_i, \alpha_i, \beta_i\}$ that previously resulted in the negative values of M. We repeatedly solve Equations (3) and (4). Remarkably, the computed value of M exhibits oscillations, frequently transitioning to positive values across multiple trials. This observation illustrates that the minimum value of F_4 is effectively zero within the numerical-uncertainty tolerance. Consequently, this provides evidence that the entropic fill F_4 satisfies the stronger version of local monotonicity for four-qubit pure states.

Now that we have confirmed that the quantity F_4 meets all criteria, (A) the "genuine" requirement, (B) additivity, and (C) local monotonicity, we claim that the entropic fill F_4 derived from the volume of the entropic tetrahedron is a proper four-qubit entanglement measure.

For a visual demonstration of entropic tetrahedra for different types of states, refer to Figure 3. The caption provides detailed explanations.

States	$\|1234\rangle$	$\|1\rangle \otimes \|234\rangle$	$\|12\rangle \otimes \|34\rangle$	$\|1\rangle \otimes \|2\rangle \otimes \|34\rangle$	$\|1\rangle \otimes \|2\rangle \otimes \|3\rangle \otimes \|4\rangle$
Separabilities	Genuinely entangled	One–to–other biseparable	Two–to–other biseparable	One–one–two biseparable	Product
Tetrahedra	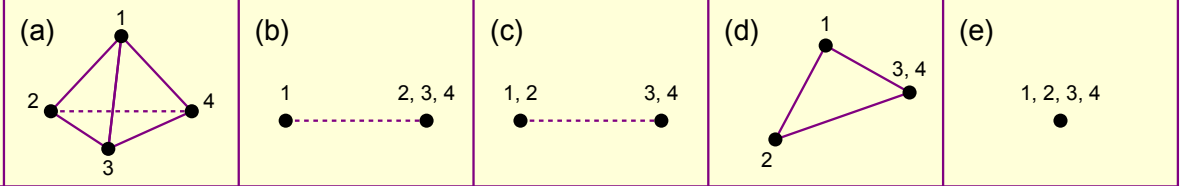				
Volumes	> 0	= 0	= 0	= 0	= 0

Figure 3. Entropic tetrahedra for different types of four-qubit states. (**a**) The tetrahedron for a genuinely entangled state has a positive volume. (**b**) The tetrahedron for a one-to-other biseparable state is an infinitely long line with zero volume, represented by the dashed line. (**c**) The tetrahedron for a two-to-other biseparable state is also an infinitely long line with zero volume, represented by the dashed line. (**d**) The tetrahedron for a one-one-two biseparable state is a coplanar triangle with zero volume. It is interesting to note that this is the only case where the shape of the tetrahedron is not fixed, as long as the area of the triangle is equal to the bipartite entropy E_{34}. (**e**) The tetrahedron for a product state is a dot with zero volume.

5. Permutation Invariance of Quantum Parties

Entropic fill derives from the bipartite entropies $\{E_{i(jkl)}, E_{(ij)(kl)}\}$. We note that these values induce two additional entanglement measures through algebraic constructions: one being their minimum, labeled as "MIN", and the other being their geometric mean, labeled as "GM." Constructions within these approaches can be found in [9,28,30–32]. Importantly, the two algebraic measures MIN and GM also satisfy the above three criteria (A), (B), and (C), establishing them as two additional entanglement measures. Next, we compare these three measures.

In four-qubit systems, the Greenberger–Horne–Zeilinger (GHZ) state $(|0000\rangle + |1111\rangle)/\sqrt{2}$ and the cluster state $|\phi_4\rangle = (|0000\rangle + |0011\rangle + |1100\rangle - |1111\rangle)/2$ are two famous examples of highly entangled states [33]. These two states possess different entanglement properties and are used for different quantum tasks, so it is not straightforward to determine their entanglement ranking. Interestingly, we find that the above three measures give three entirely different entanglement rankings for the two states, as illustrated in Table 1.

Table 1. Bipartite entanglement entropies, their minimum (labeled as MIN), their geometric mean (labeled as GM), and entropic fill F_4 for the GHZ state and the cluster state.

	$\{E_{i(jkl)}\}$	$\{E_{(ij)(kl)}\}$	**MIN**	**GM**	F_4
GHZ	{1,1,1,1}	{1,1,1}	1	1	1
cluster	{1,1,1,1}	{1,2,2}	1	1.219	0.976

Specifically, the MIN measure considers the two states as equally entangled, with $\mathrm{MIN}(\mathrm{GHZ}) = 1 = \mathrm{MIN}(\phi_4)$, as it only considers the smallest bipartite entropy, ignoring all the other details. The GM measure ranks the cluster state as more entangled, with $\mathrm{GM}(\mathrm{GHZ}) = 1 < 1.219 = \mathrm{GM}(\phi_4)$, as it multiplies all entropies together.

The entropic fill measure presents a contrasting perspective by assigning a higher entanglement value to the GHZ state, evident in $F_4(\mathrm{GHZ}) = 1 > 0.976 = F_4(\phi_4)$. This distinction arises from its geometry-based construction, and geometry is tightly linked to symmetries. To illustrate, consider that greater symmetry corresponds to a larger volume—a principle demonstrated by the fact that a sphere is the most symmetric and has the maximal volume with a fixed total surface area.

Applying this principle to our context, both the GHZ-state and the cluster-state tetrahedra share an identical total surface area. However, the tetrahedron associated with the

GHZ state has a greater volume, signaling a higher degree of symmetry. This geometric symmetry comes from the permutation invariance among parties within the quantum system. Specifically, the GHZ state remains invariant under the permutation of all four qubits. In contrast, the cluster state exhibits permutation invariance only between the first two qubits and the last two qubits. Our tetrahedron measure of entanglement successfully captures that permutation invariance.

Furthermore, from our tetrahedron measure F_4, we can define the degree of permutation invariance $\mathcal{P}$ as follows: $\mathcal{P} := F_4/F_{4,\max}^{(S)}$, where $F_{4,\max}^{(S)}$ is the maximal F_4 value with the total surface area of the entropic tetrahedron fixed by S, given by $F_{4,\max}^{(S)} = S/4$. Applying this to the two highly entangled states, we have $\mathcal{P}(\mathrm{GHZ}) = 1$ and $\mathcal{P}(\phi_4) = 0.976$.

As a further illustration, we examine the generalized GHZ states represented by $\cos\theta|0000\rangle + \sin\theta|1111\rangle$. We emphasize that, despite having varying F_4 values denoting their entanglement, these states consistently exhibit a maximal degree of permutation symmetry, $\mathcal{P} = 1$, for all possible angles of θ. This observation serves as a validation of the suitability for our defined quantity $\mathcal{P}$, as these states inherently exhibit permutation invariance among all four qubits.

6. Further Discussions

6.1. Scalability

Continuing along the geometric journey, the generalization to systems with five or more qubits presents an intriguing direction for future exploration, involving hypervolume of simplices in dimensions larger than three, making it challenging to obtain an intuitive visual representation.

Nonetheless, our tetrahedron measure presented in this work maintains its scalability. Specifically, we can consistently partition a large system into four groups and explore genuine quadripartite entanglement among these groups. Essentially, the tetrahedron measure is a genuine four-qudit entanglement measure, where each party possesses more than two dimensions. The extension of entropic fill to qudit systems has been made possible by a recent study [34]. Additionally, we have conducted numerical verifications, demonstrating the existence of unique non-negative solutions for Equations (3) and (4) in qudit systems up to $d = 50$. Consequently, we conjecture that our tetrahedron measure is also applicable to qudit systems.

An immediate application of this result is the investigation of quantum information scrambling, a phenomenon that describes the redistribution and transformation of information within quantum many-body systems. However, previous studies of information scrambling only involved entanglement across bipartitions, overlooking the rich landscape of multipartite entanglement [35–37]. This omission comes from the absence of a suitable measure to quantify GME.

With our novel GME measure relying on symmetric properties of quantum states, we can explore various GME properties in many-body systems, both theoretically and experimentally. This can involve studying the "velocity" of GME generation, enhancing our comprehension of distinct timescales within early stages of thermalization following quantum quenches. We also anticipate the identification of new phases, such as the "GME volume law" and the "GME area law".

6.2. Mixed-State Extension

The convex-roof construction generalizes entropic fill to mixed states ρ as $F_4(\rho) = \min \sum_i p_i F_4(\psi_i)$, with the minimization taken over all pure-state realizations $\rho = \sum_i p_i |\psi_i\rangle\langle\psi_i|$. Although this method is computationally intensive, numerical techniques were developed to evaluate this quantity [38–40]. Recently, a method was proposed to estimate convex-roof-based entanglement measures in experiments [41].

6.3. Alternative Approaches

As an additional observation, we have recently become aware of a distinct yet intriguing approach involving the use of a tetrahedron for quantifying genuine quadripartite entanglement, as proposed by Guo et al. [42]. This approach bears similarity to ours in the sense that it also uses a tetrahedron, with its volume serving as a GME quantifier. However, a notable difference lies in their approach: they did not employ the entanglement polygon inequalities in Equation (1) that are crucial in our approach for the one-to-other types of entanglement. This distinction raises an intriguing question about how their approach might be adapted and extended to larger systems, thereby contributing to the ongoing geometric exploration of multipartite entanglement.

Author Contributions: Conceptualization, S.X.; Methodology, S.X.; Data curation, D.Y.; Formal analysis, S.X. and Y.M.; Investigation, S.X., D.Y. and Y.M.; Writing—original draft, S.X.; writing—review and editing, S.X. and J.H.E.; Supervision, J.H.E.; Project administration, J.H.E.; Funding acquisition, J.H.E. All authors have read and agreed to the published version of the manuscript.

Funding: This research was funded by the National Science Foundation Grants No. PHY-1505189 and No. PHY-1539859 (INSPIRE), and a competitive grant from the University of Rochester.

Institutional Review Board Statement: Not applicable.

Data Availability Statement: No new data were created or analyzed in this study. Data sharing is not applicable to this article.

Acknowledgments: The authors thank Foek T. Hioe, Sabre Kais, Gabriel T. Landi, Peter W. Milonni, and Akira Sone for valuable discussions.

Conflicts of Interest: The authors declare no conflicts of interest.

References

1. Dür, W.; Vidal, G.; Cirac, J.I. Three qubits can be entangled in two inequivalent ways. *Phys. Rev. A* **2000**, *62*, 062314.
2. Laflamme, R.; Miquel, C.; Paz, J.P.; Zurek, W.H. Perfect quantum error correcting code. *Phys. Rev. Lett.* **1996**, *77*, 198.
3. Chin, A.W.; Huelga, S.F.; Plenio, M.B. Quantum metrology in non-markovian environments. *Phys. Rev. Lett.* **2012**, *109*, 233601.
4. Karlsson, A.; Bourennane, M. Quantum teleportation using three-particle entanglement. *Phys. Rev. A* **1998**, *58*, 4394.
5. Ding, Y.; Xie, S.; Eberly, J.H. Sudden freezing and thawing of entanglement sharing in a shrunken volume. *Phys. Rev. A* **2021**, *103*, 032418.
6. Anshu, A.; Harrow, A.W.; Soleimanifar, M. Entanglement spread area law in gapped ground states. *Nat. Phys.* **2022**, *18*, 1362.
7. Block, M.; Bao, Y.; Choi, S.; Altman, E.; Yao, N.Y. Measurement-induced transition in long-range interacting quantum circuits. *Phys. Rev. Lett.* **2022**, *128*, 010604.
8. Puliyil, S.; Banik, M.; Alimuddin, M. Thermodynamic signatures of genuinely multipartite entanglement. *Phys. Rev. Lett.* **2022**, *129*, 070601.
9. Ma, Z.-H.; Chen, Z.-H.; Chen, J.-L.; Spengler, C.; Gabriel, A.; Huber, M. Measure of genuine multipartite entanglement with computable lower bounds. *Phys. Rev. A* **2011**, *83*, 062325.
10. Xie, S.; Eberly, J.H. Triangle measure of tripartite entanglement. *Phys. Rev. Lett.* **2021**, *127*, 040403.
11. Coffman, V.; Kundu, J.; Wootters, W.K. Distributed entanglement. *Phys. Rev. A* **2000**, *61*, 052306.
12. Meyer, D.A.; Wallach, N.R. Global entanglement in multiparticle systems. *J. Math. Phys.* **2002**, *43*, 4273.
13. Carvalho, A.R.R.; Mintert, F.; Buchleitner, A. Decoherence and multipartite entanglement. *Phys. Rev. Lett.* **2004**, *93*, 230501.
14. Jungnitsch, B.; Moroder, T.; Gühne, O. Taming multiparticle entanglement. *Phys. Rev. Lett.* **2011**, *106*, 190502.
15. Vedral, V.; Plenio, M.B. Entanglement measures and purification procedures. *Phys. Rev. A* **1998**, *57*, 1619.
16. Wei, T.-C.; Goldbart, P.M. Geometric measure of entanglement and applications to bipartite and multipartite quantum states. *Phys. Rev. A* **2003**, *68*, 042307.
17. Blasone, M.; Dell'Anno, F.; De Siena, S.; Illuminati, F. Hierarchies of geometric entanglement. *Phys. Rev. A* **2008**, *77*, 062304.
18. Sen, A.; Sen, U. Channel capacities versus entanglement measures in multiparty quantum states. *Phys. Rev. A* **2010**, *81*, 012308.
19. Mishra, A.; Raj, A.; Kumar, A.; Mahanti, S.; Panigrahi, P.K. Geometric genuine multipartite entanglement for four-qubit systems. *arXiv* **2022**, arXiv:2212.11690.
20. Guo, Y.; Jia, Y.; Li, X.; Huang, L. Genuine multipartite entanglement measure. *J. Phys. A Math. Theor.* **2022**, *55*, 145303.
21. Jin, Z.-X.; Tao, Y.-H.; Gui, Y.-T.; Fei, S.-M.; Li-Jost, X.; Qiao, C.-F. Concurrence triangle induced genuine multipartite entanglement measure. *Results Phys.* **2023**, *44*, 106155.
22. Qian, X.-F.; Alonso, M.A.; Eberly, J.H. Entanglement polygon inequality in qubit systems. *New J. Phys.* **2018**, *20*, 063012.
23. Xie, S.; Eberly, J. Managing the three-party entanglement challenge. *Contemp. Phys.* **2022**, *62*, 189.

24. Bennett, C.H.; DiVincenzo, D.P.; Smolin, J.A.; Wootters, W.K. Mixed-state entanglement and quantum error correction. *Phys. Rev. A* **1996**, *54*, 3824.
25. Vidal, G. Entanglement monotones. *J. Mod. Opt.* **2000**, *47*, 355.
26. Chitambar, E.; Leung, D.; Mančinska, L.; Ozols, M.; Winter, A. Everything you always wanted to know about locc (but were afraid to ask). *Commun. Math. Phys.* **2014**, *328*, 303.
27. Horodecki, R.; Horodecki, P.; Horodecki, M.; Horodecki, K. Quantum entanglement. *Rev. Mod. Phys.* **2009**, *81*, 865.
28. Ge, X.; Liu, L.; Cheng, S. Tripartite entanglement measure under local operations and classical communication. *Phys. Rev. A* **2023**, *107*, 032405.
29. Acín, A.; Andrianov, A.; Jané, E.; Tarrach, R. Three-qubit pure-state canonical forms. *J. Phys. A Math. Gen.* **2001**, *34*, 6725.
30. Hashemi Rafsanjani, S.M.; Huber, M.; Broadbent, C.J.; Eberly, J.H. Genuinely multipartite concurrence of n-qubit x matrices. *Phys. Rev. A* **2012**, *86*, 062303.
31. Schneeloch, J.; Tison, C.C.; Fanto, M.L.; Ray, S.; Alsing, P.M. Quantifying tripartite entanglement with entropic correlations. *Phys. Rev. Res.* **2020**, *2*, 043152.
32. Li, Y.; Shang, J. Geometric mean of bipartite concurrences as a genuine multipartite entanglement measure. *Phys. Rev. Res.* **2022**, *4*, 023059.
33. Briegel, H.J.; Raussendorf, R. Persistent entanglement in arrays of interacting particles. *Phys. Rev. Lett.* **2001**, *86*, 910.
34. Yang, X.; Yang, Y.-H.; Luo, M.-X. Entanglement polygon inequality in qudit systems. *Phys. Rev. A* **2022**, *105*, 062402.
35. Lewis-Swan, R.; Safavi-Naini, A.; Bollinger, J.J.; Rey, A.M. Unifying scrambling, thermalization and entanglement through measurement of fidelity out-of-time-order correlators in the dicke model. *Nat. Commun.* **2019**, *10*, 1581.
36. Choi, S.; Bao, Y.; Qi, X.-L.; Altman, E. Quantum error correction in scrambling dynamics and measurement-induced phase transition. *Phys. Rev. Lett.* **2020**, *125*, 030505.
37. Zhu, Q.; Sun, Z.-H.; Gong, M.; Chen, F.; Zhang, Y.-R.; Wu, Y.; Ye, Y.; Zha, C.; Li, S.; Guo, S.; et al. Observation of thermalization and information scrambling in a superconducting quantum processor. *Phys. Rev. Lett.* **2022**, *128*, 160502.
38. Röthlisberger, B.; Lehmann, J.; Loss, D. Numerical evaluation of convex-roof entanglement measures with applications to spin rings. *Phys. Rev. A* **2009**, *80*, 042301.
39. Eisert, J.; Brandao, F.G.; Audenaert, K.M. Quantitative entanglement witnesses. *New J. Phys.* **2007**, *9*, 46.
40. Xie, S.; Younis, D.; Eberly, J.H. Sudden death of genuine tripartite entanglement. *arXiv* **2022**, arXiv:2210.01854.
41. Xie, S.; Zhao, Y.-Y.; Zhang, C.; Huang, Y.-F.; Li, C.-F.; Guo, G.-C.; Eberly, J.H. Experimental examination of entanglement estimates. *Phys. Rev. Lett.* **2023**, *130*, 150801.
42. Guo, M.-L.; Jin, Z.-X.; Li, B.; Fei, S.-M. Tetrahedron genuine entanglement measure of four-qubit systems. *J. Phys. A Math. Theor.* **2023**, *56*, 315302.

Disclaimer/Publisher's Note: The statements, opinions and data contained in all publications are solely those of the individual author(s) and contributor(s) and not of MDPI and/or the editor(s). MDPI and/or the editor(s) disclaim responsibility for any injury to people or property resulting from any ideas, methods, instructions or products referred to in the content.